

Reconstruction of heavy quark current correlators at $\mathcal{O}(\alpha_s^3)$

Y. Kiyo^a, A. Maier^a, P. Maierhöfer^a, P. Marquard^a

^a*Institut für Theoretische Teilchenphysik, Universität Karlsruhe, Karlsruhe Institute of Technology (KIT), 76128 Karlsruhe, Germany*

Abstract

We construct approximate formulas for the $\mathcal{O}(\alpha_s^3)$ QCD contributions to vector, axial-vector, scalar and pseudo-scalar quark current correlators, which are valid for arbitrary values of momenta and masses. The derivation is based on conformal mapping and the Padé approximation procedure and incorporates known expansions in the low energy, threshold and high energy regions. We use our results to estimate additional terms in these expansions.

Key words: Perturbative Calculations, Quantum Chromodynamics, Heavy Quarks
PACS: 12.38.Bx, 12.38.-t, 14.65.Dw, 14.65.Fy, 14.65.Ha

1 Introduction

Correlators of heavy quark currents in different kinematical regions are of interest for a number of phenomenological applications. These two-point functions only depend on two scales, namely the square of the external four-momentum q^2 and the heavy quark mass m . Many of the applications focus on one of three distinct kinematical regions: The low energy region with $q^2 \approx 0$, the quark pair production threshold at $q^2 = 4m^2$ and the (euclidean) high energy region $-q^2 \rightarrow \infty$.

Moments in the low energy expansion can be used for precise extractions of charm and bottom quark masses via sum rules [1] (for reviews see [2,3,4]), whereas threshold and high energy expansions are directly related to production cross sections for $t\bar{t}$, charmed hadrons or bottom hadrons in the respective energy regions.

The aforementioned expansions for the correlators in the three regions are known relatively well: In the low energy region at $\mathcal{O}(\alpha_s^2)$ the leading eight coefficients were computed more than ten years ago [5,6,7], and as of today as many as 30 moments are known [8,9]. At $\mathcal{O}(\alpha_s^3)$, however, only the first physical moment proportional to $(q^2)^1$ for axial-vector and scalar correlators [10] and the first and second moment for the pseudo-scalar and vector correlators [10,11,12,13] have been available until recently. The third moment for all four current correlators and the fourth moment for the pseudo-scalar correlator are computed in Ref. [14].

Threshold expansions for correlators are expansions in the small heavy quark velocity $v = \sqrt{1 - 4m^2/q^2} \ll 1$. Currently all of the necessary machinery for NNLO threshold expansion is known (see for instance Ref. [15] and references therein). This means, that all terms of order $(\alpha_s^n/v^{n-1}) \cdot \{1, v, v^2\}$ are in principle known for all correlators. Explicit expansions for the axial-vector, scalar and vector correlators can be derived from Refs. [16,17,18] (see Appendix A).

For high energies the leading five coefficients in the expansion are known at $\mathcal{O}(\alpha_s^2)$ for the case of scalar and pseudo-scalar currents [19] while for the vector and axial-vector currents seven terms are available [20,21]. At order α_s^3 the first two terms in the high energy expansion of the vector correlator have been published in Refs. [22,23]. More information is available for the absorptive parts of the correlators, which correspond to the logarithmic terms in the high energy expansions. Here the first three coefficients are known for the vector and axial-vector correlators [24,25,26,27,28]. The leading term in the absorptive part has been computed recently for the vector and scalar correlators [23,29,30] even at order α_s^4 .

Still, it would be desirable to have results for the correlators which are valid for arbitrary energies in addition to these expansions. One obvious benefit would be the possibility to expand such a result in a kinematical region of interest in order to obtain even more coefficients in the expansion. It would also be possible to predict values of cross sections for intermediate regions between threshold and high energies, where the mere expansions may not be very accurate anymore. Last but not least, the full energy dependence is essential for those QCD sum rule approaches to quark mass determination which use either the Borel transformation of the correlator [1] or so-called contour-improved perturbation theory [31,32,33].

Unfortunately, analytical results which are valid for arbitrary energies only exist up to $\mathcal{O}(\alpha_s)$ [34]. Still, it is possible to reconstruct the full energy dependence approximately from the known expansions at higher orders. Using a seminumerical method based on Padé approximations [35,36,37,38,39], the correlators of all four currents were reconstructed at $\mathcal{O}(\alpha_s^2)$ [5,7,40]. Moreover, it was demonstrated in [41] that in spite of the rather low amount of infor-

mation available at $\mathcal{O}(\alpha_s^3)$ it is still viable to reconstruct the vector correlator and predict expansion coefficients with decent accuracy. Recent computations of additional terms in the expansions in the low and high energy domains [13,14] have confirmed these predictions and render the application of the approximation procedure to other correlators feasible.

In this work we use the Padé approximation method to reconstruct the vector, axial-vector, scalar and pseudo-scalar heavy quark current correlators at $\mathcal{O}(\alpha_s^3)$ and derive approximations to previously unknown expansion coefficients in the low energy, threshold and high energy regions.

This paper is structured in the following way: In Section 2 we set up our conventions and explain the general approximation method. Section 3 contains details of the application of the method to the different correlators and the choice of physically meaningful approximants. The results for the reconstructed correlators and the estimates for new expansion coefficients can be found in Section 4. In Section 5 we summarise the work and give our conclusions.

2 Methods

2.1 Polarisation functions

It is convenient to explicitly extract the Lorentz structure of the heavy quark current correlators and define polarisation functions $\Pi^\delta(q^2)$, $\Pi_L^\delta(q^2)$:

$$(-q^2 g_{\mu\nu} + q_\mu q_\nu) \Pi^\delta(q^2) + q_\mu q_\nu \Pi_L^\delta(q^2) = i \int dx e^{iqx} \langle 0 | T j_\mu^\delta(x) j_\nu^\delta(0) | 0 \rangle \quad (1)$$

for $\delta = v, a$,

$$q^2 \Pi^\delta(q^2) = i \int dx e^{iqx} \langle 0 | T j^\delta(x) j^\delta(0) | 0 \rangle \quad (2)$$

for $\delta = s, p$,

where the currents are defined as

$$j_\mu^v = \bar{\psi} \gamma_\mu \psi, \quad j_\mu^a = \bar{\psi} \gamma_\mu \gamma_5 \psi, \quad j^s = \bar{\psi} \psi, \quad j^p = i \bar{\psi} \gamma_5 \psi. \quad (3)$$

The longitudinal polarisation functions $\Pi_L^\delta(q^2)$ will not be considered any further in this work: $\Pi_L^a(q^2)$ is closely related to the pseudo-scalar polarisation function $\Pi^p(q^2)$ by a Ward identity and $\Pi_L^v(q^2)$ even vanishes identically. We do not take into account singlet contributions originating from diagrams with

massless cuts¹ and choose the normalisation

$$\Pi^\delta(0) = 0. \quad (4)$$

The perturbative expansions of the polarisation functions read

$$\Pi^\delta = \Pi^{(0),\delta} + C_F \Pi^{(1),\delta} \frac{\alpha_s}{\pi} + \Pi^{(2),\delta} \left(\frac{\alpha_s}{\pi} \right)^2 + \Pi^{(3),\delta} \left(\frac{\alpha_s}{\pi} \right)^3 + \dots, \quad (5)$$

where $C_F = \frac{4}{3}$ is the quadratic Casimir operator for the adjoint representation. A natural variable to describe the behaviour of Π^δ is given by

$$z = \frac{q^2}{4m^2}, \quad (6)$$

where m denotes the heavy quark mass defined in the on-shell scheme.

For the construction of approximants we need expansions in the low energy, threshold and euclidean high energy regions, which correspond to $z = 0, 1$ and $-\infty$ respectively. Around $z = 0$ the expansion reads

$$\Pi^{(i),\delta}(z) = \frac{3}{16\pi^2} \sum_{n=1}^{\infty} C_n^{(i),\delta} z^n. \quad (7)$$

The renormalisation scale μ is set to m , so that the coefficients $C_n^{(i),\delta}$ are simply real numbers.

Around $z = 1$ we have

$$\Pi^{(i),\delta}(z) = \sum_{k=k_0}^{\infty} \sum_{l \geq 0} K_{\frac{k}{2}l}^{(i),\delta} (1-z)^{\frac{k}{2}} \log^l(1-z). \quad (8)$$

The lower bound k_0 of the sum is $3-i$ for the axial-vector and scalar correlators and $1-i$ for the vector and pseudo-scalar correlators. In the naïve Taylor series we omit the second index, i.e. $K_{\frac{k}{2}l}^{(i),\delta} \equiv K_{\frac{k}{2}0}^{(i),\delta}$

Finally, for $z \rightarrow -\infty$ we define

$$\Pi^{(i),\delta}(z) = \sum_{n=0}^{\infty} \sum_{l \geq 0} D_{nl}^{(i),\delta} \left(\frac{1}{z} \right)^n \log^l(-4z), \quad (9)$$

where we again use the convention $D_n^{(i),\delta} \equiv D_{n0}^{(i),\delta}$.

¹ The $\mathcal{O}(\alpha_s^2)$ singlet contributions and Padé approximations to them are discussed in Ref. [40].

2.2 Padé approximation

The Padé approximant $p_{n,m}(x)$ to a function f is defined as

$$p_{n,m}(x) = \frac{\sum_{i=0}^n a_i x^i}{1 + \sum_{i=1}^m b_i x^i}. \quad (10)$$

The coefficients a_i, b_i are usually fixed by imposing $n + m + 1$ conditions of the form

$$p_{n,m}^{(j)}(x_i) = f^{(j)}(x_i), \quad (11)$$

where $f^{(j)}$ is the j -th derivative of f . As long as all constraints have this form, a unique solution for the coefficients a_i, b_i is guaranteed [35].

A naïve application of the Padé approximation method will, however, fail for the functions $\Pi^{(i),\delta}(z)$ because contrary to the Padé approximants (Eq. (10)) they are not meromorphic everywhere in the complex plane. There are two major aspects of this problem, which have to be considered:

- The functions $\Pi^{(i),\delta}(z)$ diverge logarithmically for $z \rightarrow -\infty$. There are also logarithmic contributions at threshold.
- There is a branch cut along the real axis starting from $z = 1$.

This behaviour can obviously not be reproduced accurately by a Padé approximation.

The first problem related to the appearance of logarithms can be cured by splitting $\Pi^{(i),\delta}(z)$ into two parts,

$$\Pi^{(i),\delta}(z) = \Pi_{reg}^{(i),\delta}(z) + \Pi_{log}^{(i),\delta}(z), \quad (12)$$

so that $\Pi_{log}^{(i),\delta}(z)$ is a suitable function containing all known logarithmic contributions to $\Pi^{(i),\delta}(z)$. In this way the problem reduces to finding an approximation to $\Pi_{reg}^{(i),\delta}(z)$.

In the case of the vector and axial-vector polarisation functions, the functions $\Pi^{(i),\delta}(z)$ with $i > 1$ also show the well-known Coulomb singularity at threshold in addition to the logarithmic behaviour. Being proportional to $(1 - z)^{(1-i)/2}$ this singularity is, however, meromorphic and can be incorporated into the construction of the Padé approximants.

The second problem related to the branch cut is treated in a different way: We map the complex plane (including its cut) onto the unit circle in such a way that the branch cut is mapped onto the perimeter (see Fig. 1). This can

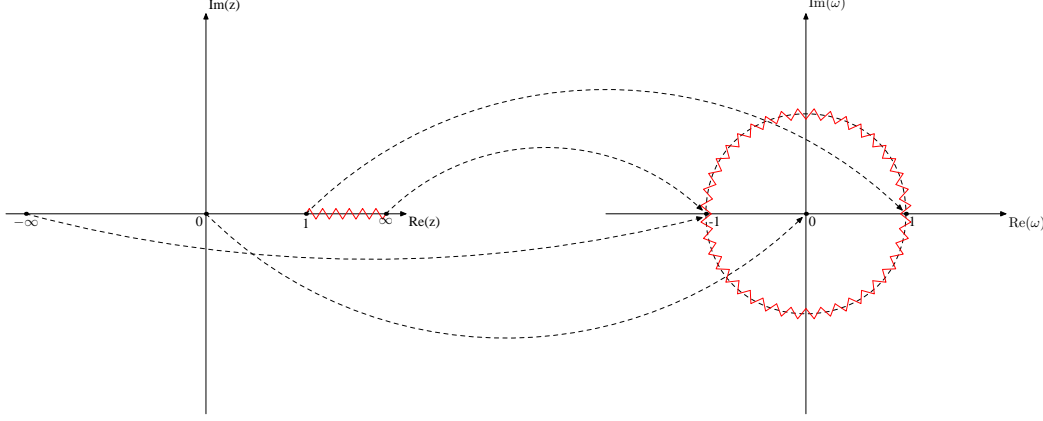


Fig. 1. Conformal mapping of the complex plane onto the unit circle. The points $z = 0$ and $z = 1$ correspond to $\omega = 0$ and $\omega = 1$, respectively. $z \pm \infty$ goes to $\omega = -1$. The branch cut starting at $z = 1$ is mapped onto the perimeter of the circle.

be achieved via the conformal transformation

$$z \rightarrow \frac{4\omega}{(1 + \omega)^2}. \quad (13)$$

The functions $\Pi_{reg}^{(i),\delta}(\omega)$ are now suitable for the Padé approximation procedure.

In the next step we fix the coefficients a_i, b_i in Eq. (10). From the expansions in the low energy, threshold and euclidean high energy regions we know the values of the $\Pi^{(i),\delta}(z)$ and some of their derivatives for $z = 0$, $z = 1$, and $z \rightarrow -\infty$. While the information from the first two regions can be used directly to fix the derivatives of $\Pi_{reg}^{(i),\delta}(\omega)$ at $\omega = 0$ and $\omega = 1$, respectively, the expansion around $z \rightarrow -\infty$ is quite different from the expansion around $\omega = -1$.

In order to also incorporate the information from the high energy region one can use the following auxiliary function [40]

$$P_n(\omega) = \frac{(4\omega)^{n-1}}{(1 + \omega)^{2n}} \left(\Pi_{reg}^{(i),\delta}(\omega) - \sum_{j=0}^{n-1} \frac{(1 + \omega)^{2j}}{(4\omega)^j} \frac{1}{j!} \left(\frac{d}{d(1/z)} \right)^j \Pi_{reg}^{(i),\delta}(z) \Big|_{z=-\infty} \right), \quad (14)$$

where n is the highest known power of $1/z$ in the high energy expansion. $P_n(-1)$ corresponds to the coefficient of $1/z^n$, while all other terms in the expansion of $\Pi_{reg}^{(i),\delta}(z)$ around $z \rightarrow -\infty$ together with the terms from the low energy expansion determine the behaviour of $P_n(\omega)$ around $\omega = 0$. If the expansion around $z = 0$ is available up to z^m the values $P_n(0), P'_n(0), \dots, P_n^{(n+m-1)}(0)$ together with $P_n(-1)$ can be used for the construction of Padé approximants. Additional knowledge about the l leading terms in the threshold expansion translates into $P_n(1), P'_n(1), P''_n(1), \dots, P_n^{(l-1)}(1)$.

Note that the construction Eq. (14) in general produces half-integer powers of $1/z$ in the high energy expansion of the reconstructed function $\Pi_{reg}^{(i),\delta}(z)$.

Since only terms with integer powers of $1/z$ may appear in the expansion, we explicitly require that the terms with half-integer powers vanish. These additional constraints do not have the form of Eq. (11). As a result, the solution to the system of equations which determines the coefficients of the Padé approximant is, in general, no longer unique.

The Coulomb singularity proportional to $(1-z)^{(1-i)/2}$, which appears in the vector and the axial-vector correlator, can easily be incorporated by defining $P_n(\omega)$ with an additional factor $(1-\omega)^{1-i}$ on the right hand side of Eq. (14) so that the limit $\omega \rightarrow 1$ becomes regular.

3 Reconstruction of polarisation functions

In this Section we explain the details of our calculation and list the input from known expansions.

3.1 Subtractions

As explained in Section 2.2, the first step consists of absorbing the logarithmic contributions in the high energy and threshold expansions into a function $\Pi_{log}^{(3),\delta}(z)$. This function must be chosen carefully in order not to introduce undesired additional singularities in $\Pi_{reg}^{(3),\delta}(z)$. It is very convenient to use lower order analytical results as auxiliary functions [41,39], namely

$$\Pi^{(0),v}(z) = \frac{3}{16\pi^2} \left(\frac{20}{9} + \frac{4}{3z} - \frac{4(1-z)(1+2z)}{3z} G(z) \right), \quad (15)$$

$$\begin{aligned} \Pi^{(1),v}(z) = \frac{3}{16\pi^2} & \left[\frac{5}{6} + \frac{13}{6z} - (1-z) \frac{3+2z}{z} G(z) + (1-z) \frac{1-16z}{6z} G(z)^2 \right. \\ & \left. - \frac{1+2z}{6z} \left(1 + 2z(1-z) \frac{d}{dz} \right) \frac{I(z)}{z} \right], \quad (16) \end{aligned}$$

with

$$\begin{aligned} I(z) = & 6 \left(\zeta_3 + 4 \text{Li}_3(-u) + 2 \text{Li}_3(u) \right) - 8 \left(2 \text{Li}_2(-u) + \text{Li}_2(u) \right) \log(u) \\ & - 2 \left(2 \log(1+u) + \log(1-u) \right) \log(u)^2, \quad (17) \end{aligned}$$

$$G(z) = \frac{1}{2z} \frac{\log(u)}{\sqrt{1-\frac{1}{z}}}, \quad u = \frac{\sqrt{1-\frac{1}{z}}-1}{\sqrt{1-\frac{1}{z}}+1}. \quad (18)$$

First, we treat the logarithmic behaviour at threshold. The relevant expansions of the four correlators read

$$\begin{aligned}
\Pi^{(3),v}(z) &= \frac{2.63641}{1-z} + \frac{-27.2677 + 0.678207n_l}{\sqrt{1-z}} + K_0^{(3),v} \\
&\quad + (-9.47414 + 0.574190n_l) \frac{\log(1-z)}{\sqrt{1-z}} \\
&\quad + (-17.5557 + 2.37068n_l - 0.0690848n_l^2) \log(1-z) \\
&\quad + (1.31710 + 0.0312341n_l + 0.00194703n_l^2) \log(1-z)^2 \\
&\quad + (-0.630208 + 0.0763889n_l - 0.00231481n_l^2) \log(1-z)^3 \\
&\quad + \mathcal{O}(\sqrt{1-z}), \\
\Pi^{(3),p}(z) &= \frac{2.63641}{1-z} + \frac{-24.9710 + 0.678207n_l}{\sqrt{1-z}} + K_0^{(3),p} \\
&\quad + (-9.47414 + 0.574190n_l) \frac{\log(1-z)}{\sqrt{1-z}} \\
&\quad + (-10.9576 + 2.56218n_l - 0.0690848n_l^2) \log(1-z) \\
&\quad + (3.23760 + 0.00345635n_l + 0.00194703n_l^2) \log(1-z)^2 \\
&\quad + (-0.630208 + 0.0763889n_l - 0.00231481n_l^2) \log(1-z)^3 \\
&\quad + \mathcal{O}(\sqrt{1-z}), \\
\Pi^{(3),a}(z) &= -0.731082 \log(1-z) + K_0^{(3),a} + \mathcal{O}(\sqrt{1-z}), \\
\Pi^{(3),s}(z) &= -1.09662 \log(1-z) + K_0^{(3),s} + \mathcal{O}(\sqrt{1-z}), \tag{19}
\end{aligned}$$

where n_l is the number of light quarks. The corresponding analytic expressions and a brief outline of the derivation of the expansions can be found in Appendix A.

The construction of $\Pi_{\log}^{(3),\delta}(z)$ is based on the expansions of $\Pi^{(1),v}$ and $G(z)$ in the threshold region:

$$G(z) = \frac{\pi}{2} \frac{1}{\sqrt{1-z}} + \mathcal{O}((1-z)^0), \tag{20}$$

$$\Pi^{(1),v}(z) = -\frac{3}{16} \log(1-z) + \text{const} + \mathcal{O}(\sqrt{1-z}). \tag{21}$$

Obviously, we can obtain logarithms from $\Pi^{(1),v}(z)$ and powers of $\frac{1}{\sqrt{1-z}}$ from $G(z)$. Therefore, as a first attempt, we choose $\Pi_{\log}^{(3),\delta}(z)$ to be a linear combination of the form

$$\Pi_{\log}^{(3),\delta}(z) = \sum_{i>0, j} k_{ij} \Pi^{(1),v}(z)^i G(z)^j. \tag{22}$$

This choice of $\Pi_{\log}^{(3),\delta}(z)$ will be modified later on when we consider the high energy region. The bounds of summation are chosen according to the powers of $\log(1-z)$ and $\frac{1}{\sqrt{1-z}}$ that appear in the threshold expansions of the polarisation

functions. The condition that this ansatz reproduces the known logarithmic contributions leads to a linear system of equations for the coefficients k_{ij} , which determines them uniquely.

After taking care of the threshold logarithms, we treat those appearing in the high energy expansions of the correlators²:

$$\begin{aligned}
\Pi^{(3),v}(z) = & -10.0036 + 1.37572n_l - 0.0328147n_l^2 \\
& + (-0.357488 + 0.102421n_l - 0.00218365n_l^2) \log(-4z) \\
& + (0.193107 - 0.0254675n_l + 0.000486744n_l^2) \log(-4z)^2 \\
& + (-0.0563482 + 0.00727073n_l - 0.000234540n_l^2) \log(-4z)^3 \\
& + \left[-7.11044 + 1.01908n_l - 0.0310950n_l^2 \right. \\
& + (-5.88388 + 0.753052n_l - 0.0146587n_l^2) \log(-4z) \\
& + (2.82917 - 0.251016n_l + 0.00457353n_l^2) \log(-4z)^2 \\
& \left. + (-0.416015 + 0.0344773n_l - 0.000703619n_l^2) \log(-4z)^3 \right] \frac{1}{z} \\
& + \left[D_2^{(3),v} + (-7.85787 + 0.987298n_l - 0.0260187n_l^2) \log(-4z) \right. \\
& + (0.215865 + 0.0367569n_l - 0.000883940n_l^2) \log(-4z)^2 \\
& + (0.525948 - 0.0435071n_l + 0.000674302n_l^2) \log(-4z)^3 \\
& \left. + (-0.0955383 + 0.00589281n_l - 0.0000879524n_l^2) \log(-4z)^4 \right] \frac{1}{z^2} \\
& + \mathcal{O}\left(\frac{1}{z^3}\right),
\end{aligned}$$

$$\begin{aligned}
\Pi^{(3),p}(z) = & -25.1130 + 3.48518n_l - 0.102852n_l^2 \\
& + (2.20686 - 0.230808n_l + 0.0142957n_l^2) \log(-4z) \\
& + (6.14249 - 0.637024n_l + 0.0110499n_l^2) \log(-4z)^2 \\
& + (-1.56708 + 0.135388n_l - 0.00257994n_l^2) \log(-4z)^3 \\
& + (0.104004 - 0.00861934n_l + 0.000175905n_l^2) \log(-4z)^4 \\
& + \left[-1.35821 + 0.177211n_l - 0.00711947n_l^2 \right. \\
& + (-17.9226 + 2.10947n_l - 0.0515675n_l^2) \log(-4z) \\
& + (3.44902 - 0.144872n_l + 0.00118877n_l^2) \log(-4z)^2 \\
& + (0.559407 - 0.0548237n_l + 0.000820889n_l^2) \log(-4z)^3 \\
& \left. + (-0.191077 + 0.0117856n_l - 0.000175905n_l^2) \log(-4z)^4 \right] \frac{1}{z}
\end{aligned}$$

² In the formulas below we also give some not yet published results. Namely, the first two non-logarithmic terms in the $1/z$ expansion of the scalar, pseudo-scalar and axial-vector correlators come from Ref. [42], while the logarithmic contribution of order $1/z^2$ to the scalar and pseudo-scalar correlators come from Ref. [43].

$$\begin{aligned}
& + \left[D_2^{(3),p} + (-7.80715 + 0.685314n_l - 0.0148423n_l^2) \log(-4z) \right. \\
& + (-1.79679 + 0.226979n_l - 0.00452222n_l^2) \log(-4z)^2 \\
& + (1.61678 - 0.107265n_l + 0.00148053n_l^2) \log(-4z)^3 \\
& + (-0.184997 + 0.00989465n_l - 0.000131929n_l^2) \log(-4z)^4 \left. \right] \frac{1}{z^2} \\
& + \mathcal{O}\left(\frac{1}{z^3}\right),
\end{aligned}$$

$$\begin{aligned}
\Pi^{(3),a}(z) = & -9.05417 + 1.17501n_l - 0.0275071n_l^2 \\
& + (-0.357488 + 0.102421n_l - 0.00218365n_l^2) \log(-4z) \\
& + (0.193107 - 0.0254675n_l + 0.000486744n_l^2) \log(-4z)^2 \\
& + (-0.0563482 + 0.00727073n_l - 0.000234540n_l^2) \log(-4z)^3 \\
& + \left[15.8531 - 2.36372n_l + 0.0700597n_l^2 \right. \\
& + (-5.65395 + 0.850654n_l - 0.0286846n_l^2) \log(-4z) \\
& + (-3.72933 + 0.420485n_l - 0.00717996n_l^2) \log(-4z)^2 \\
& + (1.15106 - 0.100911n_l + 0.00187632n_l^2) \log(-4z)^3 \\
& + (-0.104004 + 0.00861934n_l - 0.000175905n_l^2) \log(-4z)^4 \left. \right] \frac{1}{z} \\
& + \left[D_2^{(3),a} + (6.89148 - 0.858786n_l + 0.0213308n_l^2) \log(-4z) \right. \\
& + (-0.537351 - 0.00471280n_l + 0.000272690n_l^2) \log(-4z)^2 \\
& + (-0.444548 + 0.0443867n_l - 0.000850207n_l^2) \log(-4z)^3 \\
& + (0.0955383 - 0.00589281n_l + 0.0000879524n_l^2) \log(-4z)^4 \left. \right] \frac{1}{z^2} \\
& + \mathcal{O}\left(\frac{1}{z^3}\right),
\end{aligned}$$

$$\begin{aligned}
\Pi^{(3),s}(z) = & -32.1410 + 4.42783n_l - 0.125454n_l^2 \\
& + (2.20686 - 0.230808n_l + 0.0142957n_l^2) \log(-4z) \\
& + (6.14249 - 0.637024n_l + 0.0110499n_l^2) \log(-4z)^2 \\
& + (-1.56708 + 0.135388n_l - 0.00257994n_l^2) \log(-4z)^3 \\
& + (0.104004 - 0.00861934n_l + 0.000175905n_l^2) \log(-4z)^4 \\
& + \left[40.4451 - 5.58423n_l + 0.173022n_l^2 \right. \\
& + (-27.2831 + 3.37357n_l - 0.0984771n_l^2) \log(-4z) \\
& + (-8.17872 + 0.943070n_l - 0.0168387n_l^2) \log(-4z)^2 \\
& + (4.73545 - 0.353041n_l + 0.00527714n_l^2) \log(-4z)^3 \\
& + (-0.573230 + 0.0353569n_l - 0.000527714n_l^2) \log(-4z)^4 \left. \right] \frac{1}{z} \\
& + \left[D_2^{(3),s} + (16.9813 - 1.84595n_l + 0.0461425n_l^2) \log(-4z) \right. \\
& + (-5.04041 + 0.162549n_l + 0.00179429n_l^2) \log(-4z)^2 \\
& + (-1.58168 + 0.153983n_l - 0.00233074n_l^2) \log(-4z)^3 \\
& + (0.554991 - 0.0296839n_l + 0.000395786n_l^2) \log(-4z)^4 \left. \right] \frac{1}{z^2} \\
& + \mathcal{O}\left(\frac{1}{z^3}\right).
\end{aligned} \tag{23}$$

The high energy logarithms can be generated through $G(z)$:

$$G(z) = \frac{-\log(-4z)}{2z} + \mathcal{O}\left(\frac{1}{z^2}\right). \quad (24)$$

However, the behaviour in the threshold region must not be spoiled by additional poles induced by the threshold expansion of $G(z)$ (see Eq. (20)). The simplest way to avoid this would be to multiply $G(z)$ by a factor $\sqrt{1-z}$, which can however introduce non-integer powers of z in the high energy expansion. Following these considerations we extend the ansatz (22) to

$$\Pi_{log}^{(3),\delta}(z) = \sum_{i>0,j} k_{ij} \Pi^{(1),v}(z)^i G(z)^j + \sum_{m,n} d_{mn} (zG(z))^m \left(1 - \frac{1}{z}\right)^{\lceil \frac{m}{2} \rceil} \frac{1}{z^n}, \quad (25)$$

where $\lceil \dots \rceil$ means rounding up to the next integer number. The coefficients d_{mn} with $m > 0$ are again fixed by demanding that the known logarithms of $\Pi^{(3),\delta}$ are reproduced correctly up to the highest known order. This leads to singular terms in the low energy expansion of $\Pi_{log}^{(3),\delta}(z)$. We adjust the coefficients d_{0n} in such a way that these singular terms are cancelled. Furthermore we can retain the property $\Pi_{reg}^{(3),\delta}(0) = 0$, which also means $\Pi_{log}^{(3),\delta}(0) = 0$ by Eq. (12), by choosing the remaining free coefficient d_{00} accordingly.

The choice of $\Pi_{log}^{(3),\delta}(z)$ is of course not unique. A perfect reconstruction of the polarisation function would clearly not depend on the specific choice, so variations of $\Pi_{log}^{(3),\delta}(z)$ can be used to estimate the quality of the approximation procedure. Following Ref. [41], we introduce additional parameters a_i and b_i for this purpose. For the vector and pseudo-scalar correlators we modify the ansatz Eq. (25) for $\Pi_{log}^{(3),\delta}(z)$ in the following way: In the first sum, we multiply the summands with $i = 3, j = 0$ and $i = j = 1$ (which roughly correspond to terms proportional to $\log^3(1-z)$ and $\log(1-z)/\sqrt{1-z}$) by factors $a_1 + 1/z$ and $a_2 + 1/z$, respectively. In the second sum all summands corresponding to the two highest powers of logarithms are multiplied by factors $1 + 1/(b_1z)$ for $m = 3$ and $1 + 1/(b_2z)$ for $m = 4$.

In the cases of the axial-vector and scalar correlator the threshold behaviour is quite different and only one term proportional to $\log(1-z)$ is known. Consequently the first sum in the ansatz Eq. (25) for $\Pi_{log}^{(3),\delta}(z)$ shrinks to a single term. This term is multiplied by $a_1 + 1/z$. In order to arrive at a total number of four parameters like in the vector and pseudo-scalar case, we multiply the terms corresponding to the three highest powers of logarithms in the second sum by factors $1 + 1/(b_1z)$, $1 + 1/(b_2z)$ and $1 + 1/(b_3z)$.

Except for the conditions $a_i \neq -1$ and $b_i \neq 0$ the values of the parameters are

in principle arbitrary. We vary them independently with

$$\begin{aligned} a_i &\in \{-1 \pm 1, -1 \pm 4, -1 \pm 16, -1 \pm 64\}, \\ b_i &\in \{\pm 1, \pm 4, \pm 16, \pm 64\}. \end{aligned} \quad (26)$$

3.2 Padé approximation

In the next step we determine the coefficients of the Padé approximants from the expansions in the low energy, threshold, and euclidean high energy region. The low energy expansions are taken from [14]; in numerical form they read

$$\begin{aligned} \Pi^{(3),v}(z) &= (10.6103 - 1.30278n_l + 0.0282783n_l^2)z \\ &\quad + (10.4187 - 1.12407n_l + 0.0223706n_l^2)z^2 \\ &\quad + (10.2031 - 1.01971n_l + 0.0194021n_l^2)z^3 + \mathcal{O}(z^4), \\ \Pi^{(3),p}(z) &= (0.812723 - 0.190853n_l + 0.00721861n_l^2)z \\ &\quad + (6.33595 - 0.693155n_l + 0.0145600n_l^2)z^2 \\ &\quad + (8.36076 - 0.803494n_l + 0.0154075n_l^2)z^3 \\ &\quad + (9.14377 - 0.818646n_l + 0.0149416n_l^2)z^4 + \mathcal{O}(z^5), \\ \Pi^{(3),a}(z) &= (4.84212 - 0.610731n_l + 0.0141353n_l^2)z \\ &\quad + (2.93924 - 0.335580n_l + 0.00716845n_l^2)z^2 \\ &\quad + (2.06278 - 0.222971n_l + 0.00461424n_l^2)z^3 + \mathcal{O}(z^4), \\ \Pi^{(3),s}(z) &= (0.123690 - 0.0679839n_l + 0.00455586n_l^2)z \\ &\quad + (1.78515 - 0.232769n_l + 0.00574404n_l^2)z^2 \\ &\quad + (1.92442 - 0.215014n_l + 0.00469613n_l^2)z^3 + \mathcal{O}(z^4). \end{aligned} \quad (27)$$

The expansions around threshold and for high energies are listed in Eqs. (19) and (23), respectively.

Following Ref. [41], we additionally require that terms proportional to $z^{-\frac{3}{2}}$ and $z^{-\frac{5}{2}}$ are absent in the high energy expansion. The resulting number of constraints from the different kinematic regions is listed in Table 1.

3.3 Discussion of approximants

It turns out that some of the approximants have poles inside the unit circle which translate to unphysical poles inside the complex z -plane for the reconstructed polarisation functions. For this reason we immediately discard approximants which have poles for $|\omega| < 1$.

There is an additional subtlety for poles which do not lie inside, but close

current	low energy	threshold	high energy	total
vector	3	2	2+2	9
axial-vector	3	0	2+2	7
scalar	3	0	2+2	7
pseudo-scalar	4	2	2+2	10

Table 1

Number of constraints from the various kinematical regions for the different current correlators. In the high energy region constraints from both known expansion coefficients and absence of terms with half-integer powers of $1/z$ are listed

to the unit circle. As pointed out in Ref. [41], these poles can have a huge numerical effect on the behaviour of the approximant on the perimeter of the circle. More specifically, they can lead to unphysical peaks in the cross sections derived from the imaginary parts of the polarisation functions above threshold.

To avoid such resonances we discard approximants that have pronounced maxima on the perimeter of the circle, i.e.

$$\max \left| p_{n,m}(\omega) \Big|_{|\omega|=1} \right| > \rho, \quad (28)$$

where the value of ρ is chosen heuristically using the following two criteria: first, the real and imaginary parts of the polarisation functions should show no significant additional peaks; second, an adequate number of $\mathcal{O}(1000)$ to $\mathcal{O}(10000)$ “good” approximants should remain. In practice, we choose $\rho = 3$ for the vector, scalar and pseudo-scalar correlators and $\rho = 1.2$ for the axial-vector correlator.

4 Results

From the Padé approximants we reconstruct the polarisation functions using the corresponding equations (12), (13) and (14). Their imaginary parts corresponding to hadron production cross sections are plotted above the charm threshold (i.e. with $n_l = 3$) in Fig. 2 for all four correlators. The real parts are less important from a phenomenological point of view; as an example the vector polarisation function below and above the charm threshold is shown in Fig. 3. The error in the low energy region turns out to be remarkably small. Admittedly, this is not unexpected considering the fact that the polarisation functions are analytical in this region and that there is plenty of information from low energy coefficients.

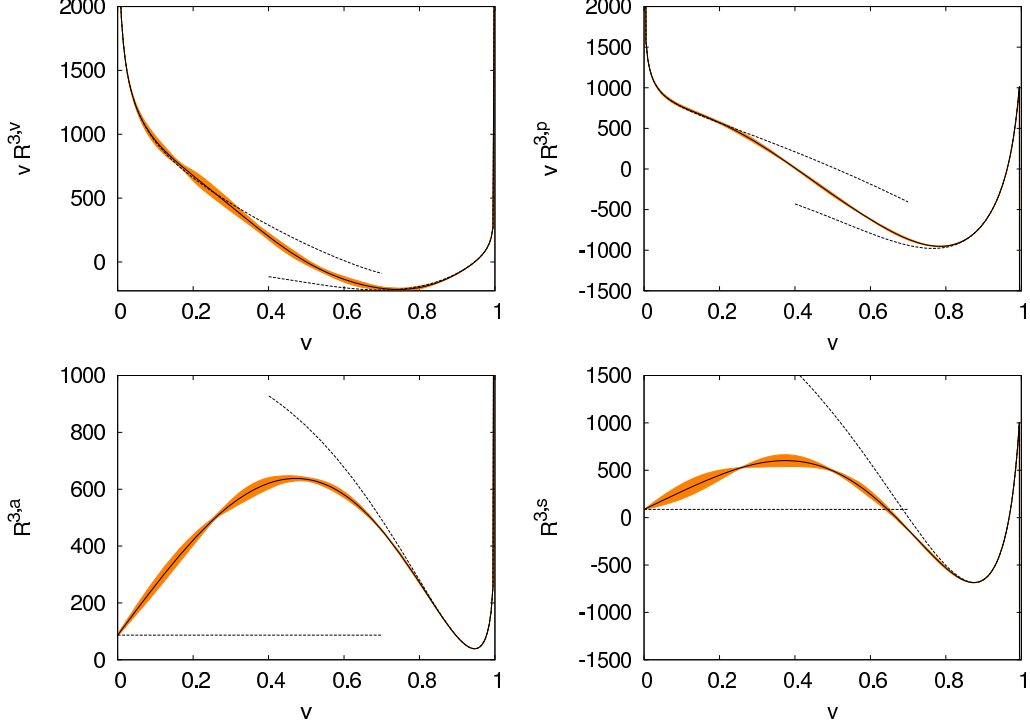


Fig. 2. Imaginary part of the four loop contributions to the vector, pseudo-scalar, axial-vector and scalar polarisation functions above the charm threshold. The plots show $vR^{(3),v} = v12\pi\text{Im}(\Pi^{(3),v})$, $vR^{(3),p} = v8\pi\text{Im}(\Pi^{(3),p})$, $R^{(3),a} = 12\pi\text{Im}(\Pi^{(3),a})$ and $R^{(3),s} = 8\pi\text{Im}(\Pi^{(3),s})$ as functions of $v = \sqrt{1 - 1/z}$. The solid black line is the mean from all approximants, the area covered by three standard deviations is shown by bands. The dashed lines show the expansions in the threshold and high energy regions (see Eqs. (19) and (23)).

A selection of “typical” Padé approximants for all four correlators with $n_l = 3, 4$ and 5 massless quarks can be downloaded from <http://www-ttp.particle.uni-karlsruhe.de/Progdata/ttp09/ttp09-17/>

The reconstructed functions can be expanded again to obtain additional low energy, threshold and high energy coefficients. We find that the values of the coefficients are strongly peaked around the mean value (for an example, see Fig. 4). As a consequence we give our errors in terms of standard deviations. As expected the error is a lot smaller for the low energy coefficients in comparison to the coefficients in the threshold and high energy regions.

There are very few coefficients in the threshold and high energy regions which differ from the mean value by more than 50 standard deviations. We discard these coefficients. The resulting estimates for the expansion coefficients are shown in Tables 2 to 5.

Comparing our predictions for the vector correlator with the previous results [41] (see Table 6), we find indications for a different sign of the threshold

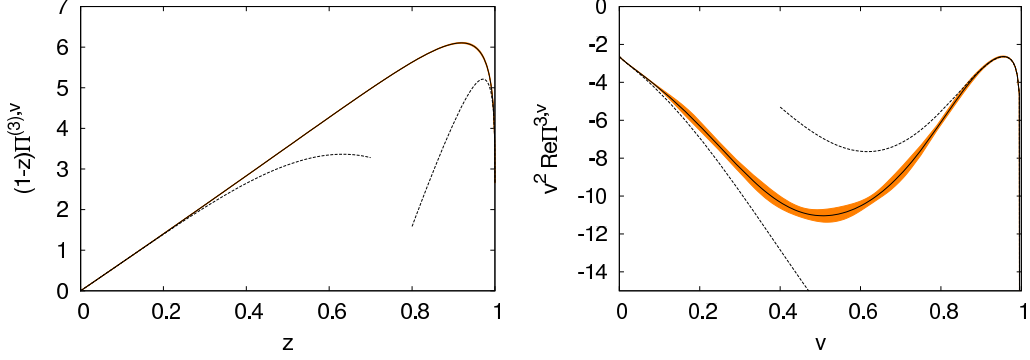


Fig. 3. Real part of the four loop contribution to the vector polarisation function for the case of charm quarks. On the left hand side the region below threshold is shown, on the right hand side the behaviour above threshold is plotted as a function of $v = \sqrt{1 - 1/z}$. The dashed lines show the known expansions in the respective regions (see Eqs. (19) and (27)), the solid lines are the mean values of all approximants. The shaded areas show the variation given by three standard deviations. In order to obtain finite values at threshold, $\text{Re}\Pi^{(3),v}$ is plotted with an extra factor $1 - z$ below and a factor v^2 above threshold.

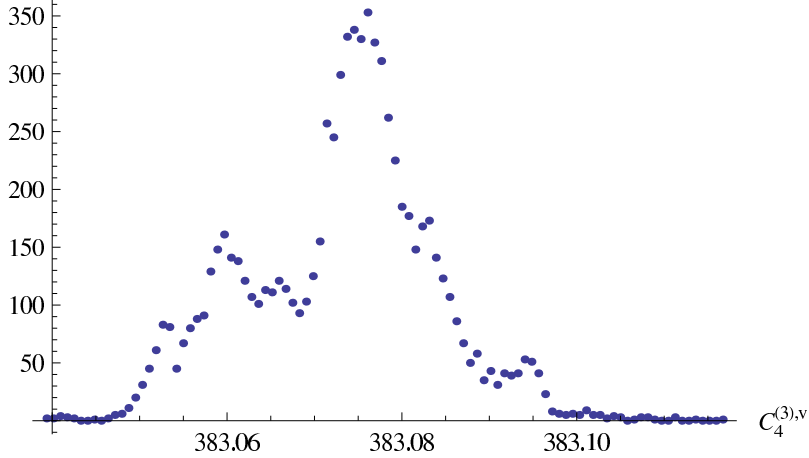


Fig. 4. Distribution of the values of $C_4^{(3),v}$ in on-shell scheme from different Padé approximants to the charm vector correlator.

constant $K_0^{(3),v}$, but good agreement for all low energy moments. Furthermore, the errors are decreased notably, depending on the coefficient by about one order of magnitude. This is mainly due to the additional information from $C_3^{(3),v}$, whereas $D_0^{(3),v}$ and $D_1^{(3),v}$ seem to play only a minor role. The impact of additional information on the quality of the predictions from the Padé approximants can also be seen in Table 7, where we compare results for the pseudo-scalar correlator with three and four low energy coefficients as input.

	$n_l = 3$	$n_l = 4$	$n_l = 5$
$C_1^{(3),v}$	366.1748	308.0188	252.8399
$C_2^{(3),v}$	381.5091	330.5835	282.0129
$C_3^{(3),v}$	385.2331	338.7065	294.2224
$C_4^{(3),v}$	383.073(11)	339.913(10)	298.576(9)
$C_5^{(3),v}$	378.688(32)	338.233(32)	299.433(27)
$C_6^{(3),v}$	373.536(61)	335.320(63)	298.622(54)
$C_7^{(3),v}$	368.23(9)	331.90(10)	296.99(9)
$C_8^{(3),v}$	363.03(13)	328.33(14)	294.94(12)
$C_9^{(3),v}$	358.06(17)	324.78(18)	292.72(16)
$C_{10}^{(3),v}$	353.35(20)	321.31(22)	290.44(19)
$K_0^{(3),v}$	17(11)	17(29)	16(10)
$D_2^{(3),v}$	2.0(42)	1.2(83)	1.4(21)

	$n_l = 3$	$n_l = 4$	$n_l = 5$
$C_1^{(3),p}$	16.0615	8.6753	2.0489
$C_2^{(3),p}$	230.9502	199.8289	170.2403
$C_3^{(3),p}$	320.5093	283.8922	248.8971
$C_4^{(3),p}$	359.1116	321.5253	285.5120
$C_5^{(3),p}$	376.3673(23)	339.2386(21)	303.6025(20)
$C_6^{(3),p}$	383.6206(84)	347.4338(75)	312.6556(70)
$C_7^{(3),p}$	385.794(18)	350.695(17)	316.925(16)
$C_8^{(3),p}$	385.250(32)	351.252(29)	318.511(28)
$C_9^{(3),p}$	383.215(48)	350.278(44)	318.533(42)
$C_{10}^{(3),p}$	380.360(66)	348.424(61)	317.620(58)
$K_0^{(3),p}$	2(76)	8(27)	11(42)
$D_2^{(3),p}$	4.98(57)	4.11(48)	3.46(45)

Table 2

Expansion coefficients from the reconstructed vector and pseudo-scalar polarisation functions for different numbers of light quarks in the on shell scheme. $C_{1-3}^{(3),v}$ and $C_{1-4}^{(3),p}$ are known exactly. The errors always apply to the last digits, i.e. 2.0(42) means an error of 4.2.

	$n_l = 3$	$n_l = 4$	$n_l = 5$
$C_1^{(3),a}$	165.1328	138.1938	112.7427
$C_2^{(3),a}$	105.1185	90.0956	75.8274
$C_3^{(3),a}$	75.5564	65.5198	55.9690
$C_4^{(3),a}$	57.7298(29)	50.4287(42)	43.4720(39)
$C_5^{(3),a}$	46.005(9)	40.397(13)	35.048(12)
$C_6^{(3),a}$	37.813(17)	33.338(24)	29.065(22)
$C_7^{(3),a}$	31.825(25)	28.151(36)	24.639(33)
$C_8^{(3),a}$	27.291(34)	24.206(48)	21.255(44)
$C_9^{(3),a}$	23.759(42)	21.123(59)	18.599(54)
$C_{10}^{(3),a}$	20.943(49)	18.658(69)	16.468(63)
$K_0^{(3),a}$	16.68(25)	14.28(48)	11.91(37)
$D_2^{(3),a}$	1.69(27)	1.26(38)	0.83(34)

	$n_l = 3$	$n_l = 4$	$n_l = 5$
$C_1^{(3),s}$	-2.0665	-3.9663	-5.3866
$C_2^{(3),s}$	59.9301	49.7941	40.2628
$C_3^{(3),s}$	69.5687	59.9811	50.8880
$C_4^{(3),s}$	64.641(14)	56.534(14)	48.819(13)
$C_5^{(3),s}$	57.168(43)	50.399(41)	43.946(39)
$C_6^{(3),s}$	50.069(81)	44.374(76)	38.941(73)
$C_7^{(3),s}$	43.95(12)	39.10(12)	34.47(111)
$C_8^{(3),s}$	38.81(16)	34.64(15)	30.65(149)
$C_9^{(3),s}$	34.52(20)	30.89(19)	27.41(184)
$C_{10}^{(3),s}$	30.93(24)	27.73(22)	24.67(216)
$K_0^{(3),s}$	17.4(11)	14.9(11)	12.6(12)
$D_2^{(3),s}$	7.7(10)	6.3(9)	5.1(8)

Table 3

Expansion coefficients from the reconstructed axial-vector and scalar polarisation functions for different numbers of light quarks in the on shell scheme. The coefficients $C_{1-3}^{(3),a}$ and $C_{1-3}^{(3),s}$ are known exactly.

	$n_l = 3$	$n_l = 4$	$n_l = 5$
$\bar{C}_1^{(3),v}$	-5.6404	-7.7624	-9.6923
$\bar{C}_2^{(3),v}$	-3.4937	-2.6438	-1.8258
$\bar{C}_3^{(3),v}$	-2.8395	-1.1745	0.4113
$\bar{C}_4^{(3),v}$	-3.349(11)	-1.386(10)	0.471(9)
$\bar{C}_5^{(3),v}$	-3.737(32)	-1.754(32)	0.104(27)
$\bar{C}_6^{(3),v}$	-3.735(61)	-1.910(63)	-0.228(54)
$\bar{C}_7^{(3),v}$	-3.39(10)	-1.85(10)	-0.46(9)
$\bar{C}_8^{(3),v}$	-2.85(13)	-1.67(14)	-0.66(12)
$\bar{C}_9^{(3),v}$	-2.22(17)	-1.47(18)	-0.91(16)
$\bar{C}_{10}^{(3),v}$	-1.65(20)	-1.37(22)	-1.30(19)

	$n_l = 3$	$n_l = 4$	$n_l = 5$
$\bar{C}_1^{(3),p}$	-1.2224	-7.2260	-12.4695
$\bar{C}_2^{(3),p}$	7.0659	6.0605	5.1954
$\bar{C}_3^{(3),p}$	14.5789	14.8438	15.1394
$\bar{C}_4^{(3),p}$	13.3278	14.3313	15.3164
$\bar{C}_5^{(3),p}$	9.9948(23)	11.4153(21)	12.7852(19)
$\bar{C}_6^{(3),p}$	6.8011(84)	8.3991(75)	9.9221(70)
$\bar{C}_7^{(3),p}$	4.311(18)	5.907(17)	7.408(16)
$\bar{C}_8^{(3),p}$	2.548(32)	4.008(29)	5.356(28)
$\bar{C}_9^{(3),p}$	1.373(48)	2.594(44)	3.690(42)
$\bar{C}_{10}^{(3),p}$	0.612(66)	1.517(61)	2.285(58)

Table 4

Coefficients from the low energy expansion of the reconstructed vector and pseudo-scalar polarisation functions for different numbers of light quarks. The coefficients are given in the $\overline{\text{MS}}$ scheme with $\mu = m$. $\bar{C}_{1-3}^{(3),v}$ and $\bar{C}_{1-4}^{(3),p}$ are known exactly.

	$n_l = 3$	$n_l = 4$	$n_l = 5$
$\bar{C}_1^{(3),a}$	-2.4297	-2.6606	-2.7958
$\bar{C}_2^{(3),a}$	-3.8059	-2.8384	-1.9120
$\bar{C}_3^{(3),a}$	-2.6066	-1.7770	-0.9920
$\bar{C}_4^{(3),a}$	-1.7688(29)	-1.1387(42)	-0.5498(39)
$\bar{C}_5^{(3),a}$	-1.144(9)	-0.692(13)	-0.278(12)
$\bar{C}_6^{(3),a}$	-0.678(17)	-0.376(24)	-0.109(22)
$\bar{C}_7^{(3),a}$	-0.344(25)	-0.166(36)	-0.022(33)
$\bar{C}_8^{(3),a}$	-0.121(34)	-0.047(48)	-0.004(44)
$\bar{C}_9^{(3),a}$	0.009(42)	-0.004(59)	-0.046(54)
$\bar{C}_{10}^{(3),a}$	0.061(49)	-0.024(69)	-0.138(63)

	$n_l = 3$	$n_l = 4$	$n_l = 5$
$\bar{C}_1^{(3),s}$	-5.4135	-7.0456	-8.1981
$\bar{C}_2^{(3),s}$	-12.9598	-11.6485	-10.3292
$\bar{C}_3^{(3),s}$	-6.6011	-5.4063	-4.2477
$\bar{C}_4^{(3),s}$	-3.972(14)	-3.002(14)	-2.073(13)
$\bar{C}_5^{(3),s}$	-2.665(43)	-1.903(41)	-1.181(39)
$\bar{C}_6^{(3),s}$	-1.843(81)	-1.265(76)	-0.723(73)
$\bar{C}_7^{(3),s}$	-1.26(12)	-0.84(12)	-0.45(11)
$\bar{C}_8^{(3),s}$	-0.82(16)	-0.54(15)	-0.29(15)
$\bar{C}_9^{(3),s}$	-0.51(20)	-0.35(19)	-0.22(18)
$\bar{C}_{10}^{(3),s}$	-0.30(24)	-0.25(22)	-0.22(22)

Table 5

Coefficients from the low energy expansion of the reconstructed axial-vector and scalar polarisation functions for different numbers of light quarks. The coefficients are given in the $\overline{\text{MS}}$ scheme with $\mu = m$. The coefficients $\bar{C}_{1-3}^{(3),a}$ and $\bar{C}_{1-3}^{(3),s}$ are known exactly.

5 Conclusion

We have used the Padé approximation method to reconstruct the full energy dependence of heavy quark correlators for vector, axial-vector, scalar and pseudo-scalar currents at order α_s^3 . As input we have used information from expansions in the low energy, threshold and high energy regions. Expanding

	$\bar{C}_3^{(3),v}$	$\bar{C}_4^{(3),v}$	$\bar{C}_5^{(3),v}$	$\bar{C}_6^{(3),v}$	$\bar{C}_7^{(3),v}$	$K_0^{(3),v}$
Ref. [41]	-3.28 ± 0.57	-4.2 ± 1.2	-5.0 ± 1.7	-5.3 ± 2.0	-5.2 ± 2.3	-10 ± 11
this work	-2.840 (exact)	$-3.349(11)$	$-3.737(32)$	$-3.735(61)$	$-3.39(10)$	$17(11)$

Table 6

Comparison of the $\overline{\text{MS}}$ low energy coefficients of the charm vector correlator with the previous results from [41]. In the second row, the maximum error is estimated, whereas the error in the third row is given in terms of standard deviations.

input	$\bar{C}_4^{(3),p}$	$\bar{C}_5^{(3),p}$	$\bar{C}_6^{(3),p}$	$\bar{C}_7^{(3),p}$	$\bar{C}_8^{(3),p}$	$K_0^{(3),p}$	$D_2^{(3),p}$
$\bar{C}_{1-3}^{(3),p}$	13.3310(91)	10.0053(286)	6.8221(567)	4.345(90)	2.596(128)	4(169)	4.98(63)
$\bar{C}_{1-4}^{(3),p}$	13.3278	9.9948(23)	6.8011(84)	4.311(18)	2.548(32)	2(76)	4.98(57)

Table 7

Comparison of results from different numbers of low energy coefficients. Shown are the predictions for the $\overline{\text{MS}}$ low energy coefficients of the $n_l = 3$ pseudo-scalar polarisation function with three and four moments used as input.

the reconstructed correlators, we have obtained predictions for additional coefficients in these expansions. We find that these predictions are fairly accurate for low energy coefficients but less precise for the coefficients in the threshold and high energy expansions.

Acknowledgements

We thank K. G. Chetyrkin, R. V. Harlander, J. H. Kühn, C. Reißer and M. Steinhauser for helpful discussions and carefully reading the manuscript. We are very grateful to P. A. Baikov, K. G. Chetyrkin, R. V. Harlander and J. H. Kühn for sharing their results with us prior to publication. We also thank A. Hoang and V. Mateu for useful correspondence concerning their work [41]. This work was supported by the Deutsche Forschungsgemeinschaft through the SFB/TR-9 ‘‘Computational Particle Physics’’. Ph. M. was supported by the Graduiertenkolleg ‘‘Hochenergiephysik und Teilchenastrophysik’’. A. M. thanks the Landesgraduiertenförderung for support.

A Threshold expansion

In this Appendix we summarise the threshold behaviour of all polarisation functions used in our paper. We derive the threshold behaviour of $\Pi^{(3),\delta}$ using Non-Relativistic QCD (NRQCD) [44,45]. For the present paper it is sufficient to obtain the results in an expansion in $(1-z)$ up to (and including) $\mathcal{O}((1-z)^0)$.

To this end we need the matching coefficients c_δ for the relation $j^\delta = c_\delta j_{\text{NR}}^\delta$ between QCD and NRQCD up to $\mathcal{O}(\alpha_s^2)$ for vector and pseudo-scalar correlators, but only up to $\mathcal{O}(\alpha_s^0)$ for axial-vector and scalar correlators. The $\mathcal{O}(\alpha_s^2)$ matching coefficients are derived in Ref. [46,47] for the vector current (see also Refs. [48,49]), and in Ref. [50] for the axial-vector current. The one-loop matching coefficients are known since long from standard QCD computation (see e.g. [50] and references therein). Heavy quark current correlators reduce to the correlators expressed in terms of NRQCD currents,

$$i \int dx e^{iqx} \langle 0 | T j^\delta(x) j^\delta(0) | 0 \rangle = c_\delta^2 i \int dx e^{iqx} \langle 0 | T j_{\text{NR}}^\delta(x) j_{\text{NR}}^\delta(0) | 0 \rangle + C_{\delta\delta}(q^2). \quad (\text{A.1})$$

The second term on the right-hand side is an analytic function of q^2 , which corresponds to the hard heavy quark loop shrunk to a point from a diagrammatic point of view. This term does not contribute to $R(q^2) \propto \text{Im}\Pi(q^2)$ due to its analyticity. For this reason it was never calculated in NRQCD and the constant $K_0^{(3),\delta}$ in the threshold expansion (8) remains unknown.

For the vector case the calculation of the correlator in NRQCD was done analytically in Ref. [51,18]. The expansion in $(1-z)$ can be easily obtained from it. For the other correlators we did not find the explicit results in the literature, thus we performed the calculation for the present work and present the result in this Appendix.

As an illustration we show several steps for the derivation of the threshold expansion for the case of the vector correlator. Other correlators can be obtained in a similar way. The QCD vector current can be matched to the one in NRQCD by

$$j_i^v(x) = e^{2imx_0} \left(c_1 + \frac{d_v}{6m} i \partial_0 \right) [\psi^\dagger \sigma_i \chi](x), \quad i = 1, 2, 3, \quad (\text{A.2})$$

where c_1 is the matching coefficient for the vector current whose explicit form can be found in the references mentioned previously, and $d_v = 1$ at the order of interest. The time component of the vector current vanishes in the rest frame of the heavy quarks with momentum $q = (q_0, \vec{0})$. Substituting the QCD current by the NRQCD current the right-hand side of Eq. (A.1) (neglecting $C_{\delta\delta}(q^2)$) is given by

$$\left(c_1 - \frac{d_v}{6m} E \right)^2 i \int dx e^{iEx_0} \langle 0 | T [\chi^\dagger \sigma_i \psi](x) [\psi^\dagger \sigma_j \chi](0) | 0 \rangle, \quad (\text{A.3})$$

where $E \equiv q_0 - 2m = \sqrt{q^2} - 2m$ and integration by parts is used to relate the derivative to E . It is well known that the correlators in NRQCD can be

mapped onto Green's functions in quantum mechanics; thus one obtains

$$i \int dx e^{iEx_0} \langle 0 | T[\chi^\dagger \sigma_i \psi](x) [\psi^\dagger \sigma_j \chi](0) | 0 \rangle = 2 N_c \delta_{ij} G(0, 0; E), \quad (\text{A.4})$$

where $N_c = 3$ is the number of colours for QCD and δ_{ij} is Kronecker's delta. The NNLO result for the Green's function is presented in Eq. (A.29) of Ref. [18]. One should expand the (NNLL) Green's function presented in that reference and retain relevant terms of interest. Furthermore UV divergences should be subtracted according to the $\overline{\text{MS}}$ scheme conforming with the definition of c_1 in order to arrive at the threshold expansion presented below.

Conventionally NRQCD computations are done using the effective coupling $\alpha_s^{(n_l)}(\mu)$ where the heavy quark is integrated out. We present our results using the pole mass m and the QCD coupling constant $\alpha_s^{(n_l+1)}(m)$ at the scale of the pole mass. Hence we re-express the effective coupling using the decoupling relation [52,53]

$$\alpha_s^{(n_l)}(m) = \alpha_s^{(n_l+1)}(m) \left(1 + d^{(2)} \left(\frac{\alpha_s^{(n_l+1)}(m)}{\pi} \right)^2 + \mathcal{O}(\alpha_s^3) \right), \quad (\text{A.5})$$

with $d^{(2)} = -7/24$. This induces a change in the vector and pseudo-scalar correlator in the coefficient of $\log(1-z)$ at order $\mathcal{O}((1-z)^0)$. The result for the vector and pseudo-scalar current correlators are given by

$$\begin{aligned} \Pi^{(3),v}(z) = & \frac{2\pi^2\zeta_3}{9(1-z)} + \left[-\frac{11\pi^3}{36} + \frac{\pi^3}{54}n_l \right] \frac{\log(1-z)}{\sqrt{1-z}} \\ & + \left[-\frac{\pi^3}{108} - \frac{11\pi^3 \log 2}{18} - \frac{11\pi\zeta_3}{3} \right. \\ & \left. + n_l \left(-\frac{5\pi^3}{162} + \frac{\pi^3 \log 2}{27} + \frac{2\pi\zeta_3}{9} \right) \right] \frac{1}{\sqrt{1-z}} \\ & + \left[-\frac{121}{192} + \frac{11}{144}n_l - \frac{1}{432}n_l^2 \right] \log^3(1-z) \\ & + \left[\frac{71}{96} + \frac{35\pi^2}{108} - \frac{121 \log 2}{32} + n_l \left(-\frac{55}{192} + \frac{11 \log 2}{24} \right) \right. \\ & \left. + n_l^2 \left(\frac{5}{432} - \frac{\log 2}{72} \right) \right] \log^2(1-z) \end{aligned}$$

$$\begin{aligned}
& + \left[-\frac{4169}{3456} - \frac{20741\pi^2}{5184} + \frac{9\pi^4}{256} + \frac{71 \log 2}{24} \right. \\
& + \frac{56\pi^2 \log 2}{27} - \frac{121 \log^2 2}{16} + \frac{1703\zeta_3}{288} \\
& + n_l \left(\frac{79}{576} + \frac{11\pi^2}{48} - \frac{55 \log 2}{48} + \frac{11 \log^2 2}{12} + \frac{13\zeta_3}{48} \right) \\
& \left. + n_l^2 \left(-\frac{25}{1296} - \frac{\pi^2}{144} + \frac{5 \log 2}{108} - \frac{\log^2 2}{36} \right) \right] \log(1-z) \\
& + K_0^{(3),v} + \mathcal{O}(\sqrt{1-z}), \\
\Pi^{(3),p}(z) = & \frac{2\pi^2\zeta_3}{9(1-z)} + \left[-\frac{11\pi^3}{36} + \frac{\pi^3}{54}n_l \right] \frac{\log(1-z)}{\sqrt{1-z}} \\
& + \left[\frac{7\pi^3}{108} - \frac{11\pi^3 \log 2}{18} - \frac{11\pi\zeta_3}{3} \right. \\
& \left. + n_l \left(-\frac{5\pi^3}{162} + \frac{\pi^3 \log 2}{27} + \frac{2\pi\zeta_3}{9} \right) \right] \frac{1}{\sqrt{1-z}} \\
& + \left[-\frac{121}{192} + \frac{11}{144}n_l - \frac{1}{432}n_l^2 \right] \log^3(1-z) \\
& + \left[\frac{115}{96} + \frac{17\pi^2}{36} - \frac{121 \log 2}{32} + n_l \left(-\frac{181}{576} + \frac{11 \log 2}{24} \right) \right. \\
& \left. + n_l^2 \left(\frac{5}{432} - \frac{\log 2}{72} \right) \right] \log^2(1-z) \\
& + \left[-\frac{539}{128} - \frac{7207\pi^2}{1728} + \frac{9\pi^4}{256} + \frac{115 \log 2}{24} \right. \\
& + 3\pi^2 \log 2 - \frac{121 \log^2 2}{16} + \frac{287\zeta_3}{32} \\
& + n_l \left(\frac{701}{1728} + \frac{11\pi^2}{48} - \frac{181 \log 2}{144} + \frac{11 \log^2 2}{12} + \frac{13\zeta_3}{48} \right) \\
& \left. + n_l^2 \left(-\frac{25}{1296} - \frac{\pi^2}{144} + \frac{5 \log 2}{108} - \frac{\log^2 2}{36} \right) \right] \log(1-z) \\
& + K_0^{(3),p} + \mathcal{O}(\sqrt{1-z}).
\end{aligned} \tag{A.6}$$

Except for the term proportional to $\log(1-z)$ the result for the vector current agrees with Ref. [41]³. The threshold behaviour for the pseudo-scalar current is new.

The scalar and axial-vector correlators are suppressed by $(1-z)$ compared to those for vector and pseudo-scalar cases. However, their leading term is

³ The overall numerical difference is very small. For α_s parametrised in terms of the $\overline{\text{MS}}$ heavy quark mass, we find full agreement with Ref.[41].

divergent, and its $1/\epsilon$ pole generates a $\log(1-z)$ in NRQCD. The result reads

$$\begin{aligned}\Pi^{(3),s}(z) &= -\frac{\pi^2}{9}\log(1-z) + K_0^{(3),s} + \mathcal{O}(\sqrt{1-z}), \\ \Pi^{(3),a}(z) &= -\frac{2\pi^2}{27}\log(1-z) + K_0^{(3),a} + \mathcal{O}(\sqrt{1-z}).\end{aligned}\quad (\text{A.7})$$

The origin of the $\log(1-z)$ is a triple insertion of Coulomb gluons which is of order $\mathcal{O}(\alpha_s^3)$ in NRQCD. The results in Eq. (A.7) are in agreement with the one in Ref. [16].

References

- [1] V. A. Novikov, et al. *Phys. Rept.*, 41:1–133, 1978.
- [2] L. J. Reinders, H. Rubinstein, S. Yazaki. *Phys. Rept.*, 127:1, 1985.
- [3] P. Colangelo, A. Khodjamirian. 2000. [hep-ph/0010175](#).
- [4] B. L. Ioffe. *Prog. Part. Nucl. Phys.*, 56:232–277, 2006. [hep-ph/0502148](#).
- [5] K. G. Chetyrkin, J. H. Kühn, M. Steinhauser. *Phys. Lett.*, B371:93–98, 1996. [hep-ph/9511430](#).
- [6] K. G. Chetyrkin, J. H. Kühn, M. Steinhauser. *Nucl. Phys.*, B482:213–240, 1996. [hep-ph/9606230](#).
- [7] K. G. Chetyrkin, J. H. Kühn, M. Steinhauser. *Nucl. Phys.*, B505:40–64, 1997. [hep-ph/9705254](#).
- [8] R. Boughezal, M. Czakon, T. Schutzmeier. *Nucl. Phys. Proc. Suppl.*, 160:160–164, 2006. [hep-ph/0607141](#).
- [9] A. Maier, P. Maierhöfer, P. Marquard. *Nucl. Phys.*, B797:218–242, 2008. [arXiv0711.2636](#).
- [10] C. Sturm. *JHEP*, 09:075, 2008. [arXiv0805.3358](#).
- [11] R. Boughezal, M. Czakon, T. Schutzmeier. *Phys. Rev.*, D74:074006, 2006. [hep-ph/0605023](#).
- [12] K. G. Chetyrkin, J. H. Kühn, C. Sturm. *Eur. Phys. J.*, C48:107–110, 2006. [hep-ph/0604234](#).
- [13] A. Maier, P. Maierhöfer, P. Marquard. *Phys. Lett.*, B669:88–91, 2008. [arXiv0806.3405](#).
- [14] A. Maier, P. Maierhöfer, P. Marquard, A. V. Smirnov. 2009. [arXiv0907.2117](#).
- [15] A. H. Hoang, et al. *Eur. Phys. J. direct*, C2:1, 2000. [hep-ph/0001286](#).

- [16] A. A. Penin, A. A. Pivovarov. *Nucl. Phys.*, B550:375–396, 1999. [hep-ph/9810496](#).
- [17] M. Beneke, A. Signer. *Phys. Lett.*, B471:233–243, 1999. [hep-ph/9906475](#).
- [18] A. Pineda, A. Signer. *Nucl. Phys.*, B762:67–94, 2007. [hep-ph/0607239](#).
- [19] R. Harlander, M. Steinhauser. *Phys. Rev.*, D56:3980–3990, 1997. [hep-ph/9704436](#).
- [20] K. G. Chetyrkin, R. Harlander, J. H. Kühn, M. Steinhauser. *Nucl. Phys.*, B503:339–353, 1997. [hep-ph/9704222](#).
- [21] R. Harlander, M. Steinhauser. *Eur. Phys. J.*, C2:151–158, 1998. [hep-ph/9710413](#).
- [22] P. A. Baikov, K. G. Chetyrkin, J. H. Kühn. *Nucl. Phys. Proc. Suppl.*, 135:243–246, 2004.
- [23] P. A. Baikov, K. G. Chetyrkin, J. H. Kühn. 2009. [arXiv0906.2987](#).
- [24] S. G. Gorishnii, A. L. Kataev, S. A. Larin. *Phys. Lett.*, B259:144–150, 1991.
- [25] L. R. Surguladze, M. A. Samuel. *Phys. Rev. Lett.*, 66:560–563, 1991 Erratum-
ibid. 66, 2416 (1991).
- [26] K. G. Chetyrkin, J. H. Kühn. *Phys. Lett.*, B248:359–364, 1990.
- [27] K. G. Chetyrkin, J. H. Kühn. *Phys. Lett.*, B406:102–109, 1997. [hep-ph/9609202](#).
- [28] K. G. Chetyrkin, R. V. Harlander, J. H. Kühn. *Nucl. Phys.*, B586:56–72, 2000. [hep-ph/0005139](#).
- [29] P. A. Baikov, K. G. Chetyrkin, J. H. Kühn. *Phys. Rev. Lett.*, 101:012002, 2008. [arXiv0801.1821](#).
- [30] P. A. Baikov, K. G. Chetyrkin, J. H. Kühn. *Phys. Rev. Lett.*, 96:012003, 2006. [hep-ph/0511063](#).
- [31] A. A. Pivovarov. *Nuovo Cim.*, A105:813–826, 1992.
- [32] A. A. Pivovarov. *Z. Phys.*, C53:461–464, 1992. [hep-ph/0302003](#).
- [33] F. Le Diberder, A. Pich. *Phys. Lett.*, B286:147–152, 1992.
- [34] A. O. G. Kallen, A. Sabry. *Kong. Dan. Vid. Sel. Mat. Fys. Med.*, 29N17:1–20, 1955.
- [35] G. A. Baker. *Essentials of Padé Approximants*. Academic Press, Inc., 1975.
- [36] D. J. Broadhurst, J. Fleischer, O. V. Tarasov. *Z. Phys.*, C60:287–302, 1993. [hep-ph/9304303](#).
- [37] J. Fleischer, O. V. Tarasov. *Z. Phys.*, C64:413–426, 1994. [hep-ph/9403230](#).

- [38] D. J. Broadhurst, et al. *Phys. Lett.*, B329:103–110, 1994. [hep-ph/9403274](#).
- [39] P. A. Baikov, D. J. Broadhurst. 1995. [hep-ph/9504398](#).
- [40] K. G. Chetyrkin, R. Harlander, M. Steinhauser. *Phys. Rev.*, D58:014012, 1998. [hep-ph/9801432](#).
- [41] A. H. Hoang, V. Mateu, S. Mohammad Zebarjad. *Nucl. Phys.*, B813:349–369, 2009. [arXiv0807.4173](#).
- [42] P. Baikov, K. Chetyrkin, J. Kühn. In preparation.
- [43] K. Chetyrkin, R. Harlander. In preparation.
- [44] W. E. Caswell, G. P. Lepage. *Phys. Lett.*, B167:437, 1986.
- [45] G. T. Bodwin, E. Braaten, G. P. Lepage. *Phys. Rev.*, D51:1125–1171, 1995. [hep-ph/9407339](#).
- [46] A. Czarnecki, K. Melnikov. *Phys. Rev. Lett.*, 80:2531–2534, 1998. [hep-ph/9712222](#).
- [47] M. Beneke, A. Signer, V. A. Smirnov. *Phys. Rev. Lett.*, 80:2535–2538, 1998. [hep-ph/9712302](#).
- [48] P. Marquard, J. H. Piclum, D. Seidel, M. Steinhauser. *Nucl. Phys.*, B758:144–160, 2006. [hep-ph/0607168](#).
- [49] P. Marquard, J. H. Piclum, D. Seidel, M. Steinhauser. *Phys. Lett.*, B678:269–275, 2009. [arXiv0904.0920](#).
- [50] B. A. Kniehl, A. Onishchenko, J. H. Piclum, M. Steinhauser. *Phys. Lett.*, B638:209–213, 2006. [hep-ph/0604072](#).
- [51] M. Beneke, A. Signer, V. A. Smirnov. *Phys. Lett.*, B454:137–146, 1999. [hep-ph/9903260](#).
- [52] S. A. Larin, T. van Ritbergen, J. A. M. Vermaseren. *Nucl. Phys.*, B438:278–306, 1995. [hep-ph/9411260](#).
- [53] K. G. Chetyrkin, B. A. Kniehl, M. Steinhauser. *Nucl. Phys.*, B510:61–87, 1998. [hep-ph/9708255](#).